

This article was downloaded by:

On: 26 January 2011

Access details: *Access Details: Free Access*

Publisher *Taylor & Francis*

Informa Ltd Registered in England and Wales Registered Number: 1072954 Registered office: Mortimer House, 37-41 Mortimer Street, London W1T 3JH, UK



Liquid Crystals

Publication details, including instructions for authors and subscription information:

<http://www.informaworld.com/smpp/title~content=t713926090>

Shapes of blue phase crystals grown in electric fields

P. Pieranski^a, P. E. Cladis^{ab}, R. Barbet-Massin^a

^a Faculté des Sciences, Laboratoire de Physique des Solides, Orsay, France ^b AT&T Bell Laboratories, Murray Hill, New Jersey, U.S.A.

To cite this Article Pieranski, P. , Cladis, P. E. and Barbet-Massin, R.(1989) 'Shapes of blue phase crystals grown in electric fields', *Liquid Crystals*, 5: 3, 829 – 838

To link to this Article: DOI: 10.1080/02678298908026388

URL: <http://dx.doi.org/10.1080/02678298908026388>

PLEASE SCROLL DOWN FOR ARTICLE

Full terms and conditions of use: <http://www.informaworld.com/terms-and-conditions-of-access.pdf>

This article may be used for research, teaching and private study purposes. Any substantial or systematic reproduction, re-distribution, re-selling, loan or sub-licensing, systematic supply or distribution in any form to anyone is expressly forbidden.

The publisher does not give any warranty express or implied or make any representation that the contents will be complete or accurate or up to date. The accuracy of any instructions, formulae and drug doses should be independently verified with primary sources. The publisher shall not be liable for any loss, actions, claims, proceedings, demand or costs or damages whatsoever or howsoever caused arising directly or indirectly in connection with or arising out of the use of this material.

Shapes of blue phase crystals grown in electric fields

by P. PIERANSKI, P. E. CLADIS† and R. BARBET-MASSIN

Laboratoire de Physique des Solides, Bâtiment 510, Faculté des Sciences,
91405 Orsay, France

By breaking spatial isotropy, an applied electric field modifies the equilibrium shapes of crystals. Only those crystal shapes whose symmetry is compatible with this reduced spatial symmetry grow. The effect is small in atomic crystals but observable in blue phase crystals which have millions of molecules per unit cell. An analysis is presented discussing electric field-induced modifications to cubic blue phase crystals. Specific examples are shown for BP II.

1. Introduction: symmetry of crystal shapes

Crystal shapes are composed of facets and/or rounded parts corresponding to a distribution of steps. Most theories of crystal shapes [1-3] deal with ideal situations where crystals are in equilibrium with an isotropic environment (for example, an isotropic liquid) or are growing in isotropic conditions. In these ideal situations the crystal shape must be invariant under all symmetry operations of a point group G_p isogonal with the space group G_s of the crystal structure.

Real crystals have facets of different sizes and shapes, determined by growth conditions, so that the overall crystal shape has symmetry G'_h lower than the symmetry G_h of the ideal crystal. In crystallographic studies these differences in the size and shapes of facets are neglected and only angular relationships between facets, which do not depend on growth conditions, are used to determine the crystal symmetry, G_s . It is clear, however, that this variable symmetry G'_h of real crystals is not arbitrary but depends in a precise manner on the symmetry, G_e , of the environment during growth.

The purpose of this paper is to analyse the change in crystal shapes of blue phases grown in the presence of a homogeneous alternating electric field E of different orientations with respect to the symmetry axes of the crystals. The electric field induces a well defined axial symmetry D_∞ (we neglect the inversion operation because blue phases are chiral) for the growth condition so that the resultant reduction of the crystal shape symmetry can be treated rigorously. The paper is organized as follows: in §2 we analyse qualitatively how the axial symmetry D_∞ of the field affects crystal shapes. In §3 we calculate the energy $\beta_{(110)}$ of steps on (110) facets of blue phases for different orientations of the electric field. Defect-free monocrystals grow uniquely by two dimensional nucleation of new crystal planes so that the step energy $\beta_{110}(E)$ determines growth rates of the (110) facets. Using a plot of a dimensionless quantity $\tilde{\beta}_a = \{[\beta(E)^4/\beta(0)^4] - 1\}$ versus the field direction we find qualitative agreement with the results of §2 as well as with experimental facts reported briefly in the final section.

2. Reduction of the symmetry of crystal shapes due to an anisotropic environment

The shape of a crystal grown under anisotropic conditions with symmetry G_e must be invariant under symmetry operations common to the group G_e and to the point

† *Permanent address:* AT&T Bell Laboratories, 600 Mountain Avenue Murray Hill, New Jersey 07974, U.S.A.

G_P of the crystal structure. These common symmetry operations form a group G_h which must be a subgroup both of G_P and G_c . The point group G_P of blue phases I and II, isogonal with their respective space groups $O^8(I4_132)$ and $O^2(P4_232)$ is $O(432)$. The symmetry of an alternating electric field E , with a frequency f much larger than any characteristic frequency f_c involved in the growth process, and acting on a chiral medium, is D_∞ . The resultant common symmetry $G_h = (G_P \cap G_c)$ depends on the orientation of the field with respect to the crystal axes.

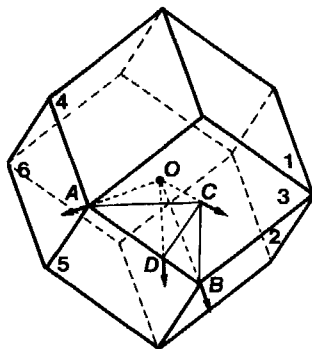


Figure 1. Crystal limited by 12 (110) facets. **OA**, **OB** and **OC** are the directions of the four-fold, three-fold and two-fold symmetry axes, respectively.

Figure 1 shows a crystal limited by 12 (110) facets. There are six visible facets, 1 to 6, and six hidden facets, 1' to 6', where n' indicates a facet opposite to the visible facet n . Without the field, all facets of the set $S = \{1, \dots, 6, 1', \dots, 6'\}$ grow with the same velocity and therefore must have identical shapes and sizes. When a field E is applied along the four-fold axis **OA**, the symmetry operations common to the groups G_P and G_c are: the four-fold axis **OA**, two two-fold axes obtained from the two other four-fold axes perpendicular to **OA**, two two-fold axes perpendicular to the facets 1 and 2 and the identity e . These operations form a group D_4 which, as required, is a subgroup of both O and D_∞ . With this reduction of symmetry, the set S of 12 facets splits into two disjoint sets $S_1^A = \{1, 2, 1', 2'\}$ and $S_2^A = \{3, 4, 5, 6, 3', 4', 5', 6'\}$ of equivalent facets. The symmetry operations of the group D_4 permute only facets belonging to the same set S_1^A or S_2^A .

The same considerations can be applied to other directions of the field such as **OB**, **OC**, **OD** and all intermediate directions forming a loop **ABCADC** shown in figure 1. The resultant symmetry reductions and splittings of the set S are summarized in the table.

Symmetry of crystal shapes in an electric field.

Direction of the field	Symmetry of the crystal shapes	Sets of equivalent facets
OA	D_4	$\{1, 2, 1', 2'\}; \{3, 4, 5, 6, 3', 4', 5', 6'\}$
(OA, OB)	C_2	$\{1\}; \{1'\}; \{2, 2'\}; \{3, 3'\}; \{5, 3'\}; \{4, 6'\}; \{6, 4'\}$
OB	D_3	$\{2, 3, 5, 2', 3', 5'\}; \{1, 6, 4'\}; \{1', 6', 4\}$
(OB, OC)	C_2	$\{6\}; \{6'\}; \{3, 3'\}; \{1, 4'\}; \{4, 1'\}; \{2, 5'\}; \{5, 2'\}$
OC	D_2	$\{3, 3'\}; \{6, 6'\}; \{1, 5, 4, 2'\}; \{4, 2, 1', 5'\}$
(OC, OA)	C_2	$\{3, 3'\}; \{1, 2'\}; \{2, 1'\}; \{4, 5'\}; \{5, 4'\}; \{6, 6'\}$
(OD, OC)	I	$\{n\}; n = 1, 2, \dots, 6, 1', \dots, 6'$

3. Energy of steps on (110) facets in a field

The energy per unit length of a step on the (110) facet, β_{110} , is a quantity crucial for problems of faceting and crystal growth. In equilibrium the singularity of the surface energy of a crystal surface perpendicular to \mathbf{m} is proportional to $\beta_{(110)}$ in the vicinity of the [110] direction. Also, in the approximation of two dimensional nucleation, the growth rate of the (110) facet decreases exponentially with the height ΔE of the nucleation barrier which is also proportional to $\beta_{(110)}$.

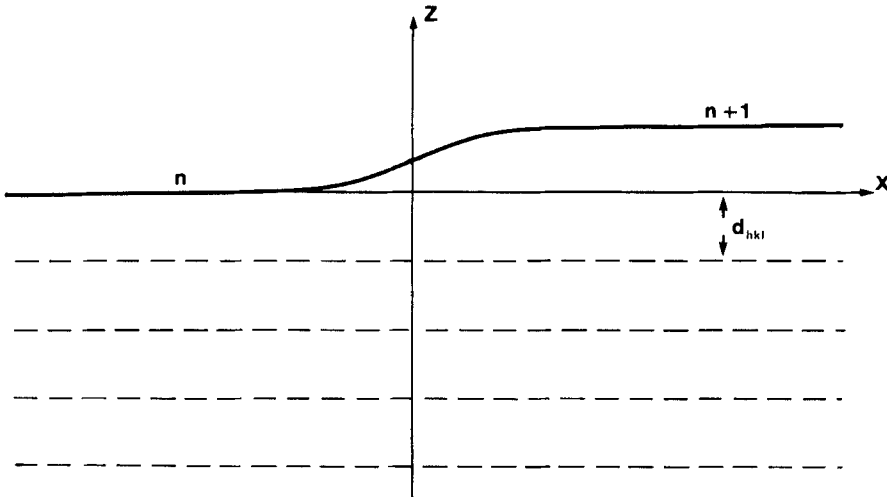


Figure 2. Model of a step on the (110) facet.

Figure 2 shows a model of the (110) crystal facet. The shape $z(x)$ of the step is found by minimizing the total surface energy, E^s :

$$E_n^s = \int \left[\frac{1}{2} \gamma_0 \left(\frac{dz}{dx} \right)^2 + V(z) \right] dx. \tag{1}$$

The first term results from an increase in the surface area due to the step. The second term is the periodic potential, from the underlying crystalline structure. It tends to fix the interface at discrete levels $z = nd_{(110)}$, where $d_{(110)}$ is the period of $V(z)$. In an electric field, $V(z)$ has two contributions

$$V(z) = V(\mathbf{0}, z) + V(\mathbf{E}, z), \tag{2}$$

where $V(\mathbf{0}, z)$ represents the periodic potential existing without the field and $V(\mathbf{E}, z)$ is the perturbation due to the field. For simplicity we set

$$V(\mathbf{0}, z) = V_0 \sin(qz + \phi_0), \tag{3}$$

where $q = 2\pi/d_{(110)}$ and ϕ_0 is the phase which depends on the choice of origin, $z = 0$. In the following we suppose that the origin is situation on a two-fold axis and the x axis of the local coordinate system (x, y, z) is parallel to it as shown in figure 3.

The perturbation $V(\mathbf{E}, z)$ can be calculated in the same manner as shown previously [4]. In blue phases I and II the anisotropic part $\hat{\epsilon}^d(\mathbf{r})$ is a periodic function of \mathbf{r} and can be expanded in a Fourier series

$$\begin{aligned} \hat{\epsilon}^d(\mathbf{r}) &= \hat{\epsilon}^d(\mathbf{r}) - \frac{1}{3} [\text{tr } \hat{\epsilon}^d(\mathbf{r})] \hat{\delta} \\ &= \sum_{\mathbf{q}} \tilde{\epsilon}(\mathbf{q}) \exp i\mathbf{q} \cdot \mathbf{r} + \text{c.c.} \end{aligned} \tag{4}$$

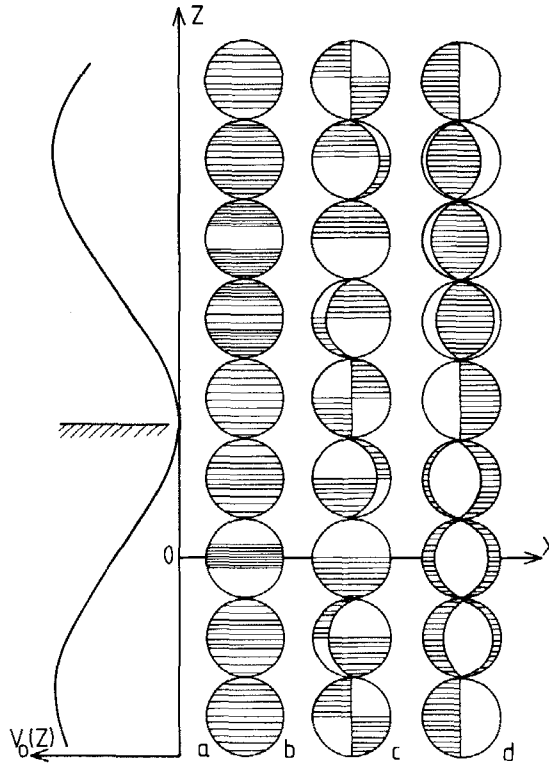


Figure 3. Choice of a local coordinate system on a (110) facet: the z axis is the two-fold symmetry axis perpendicular to the facet. The x axis coincides with a two-fold axis perpendicular to z . (a) The periodic potential $V_0(z)$; (b) $m = 0$ tensorial component of the order parameter $\hat{\varepsilon}(\mathbf{r})$; (c) 1^+ component of the order parameter; and (d) 2^+ component of the order parameter. Due to the two-fold axis z , the 1^+ component vanishes without the field and the interface tends to be fixed in a minimum of $V_0(z)$.

In an electric field \mathbf{E} the dielectric energy density

$$F^{\text{el}}(\mathbf{r}) = \frac{1}{8\pi} \mathbf{E} \cdot \varepsilon(\mathbf{r}) \cdot \mathbf{E}, \quad (5)$$

perturbs the blue phase structure. As in [4], we only consider here the low field limit where the perturbation of the order parameter $\hat{\varepsilon}(\mathbf{r})$ is small compared with its equilibrium value: $\varepsilon(\mathbf{0}, \mathbf{r})$

$$\begin{aligned} \varepsilon(\mathbf{E}, \mathbf{r}) &= \hat{\varepsilon}(\mathbf{0}, \mathbf{r}) + \delta\varepsilon(\mathbf{E}, \mathbf{r}); \\ \delta\varepsilon(\mathbf{E}, \mathbf{r}) &= O(E^2) \ll \hat{\varepsilon}(\mathbf{0}, \mathbf{r}). \end{aligned} \quad (6)$$

In this approximation each of the Fourier components of equation (4) with wave-vectors $\mathbf{q} \parallel [110]$ will contribute to $V(\mathbf{E}, z)$. Following the Landau theory of blue phases [5] we suppose that among these Fourier components the predominant one is

$$\hat{\varepsilon}_{(110)}^{2^+} = \varepsilon_{(110)}^{2^+} \begin{pmatrix} \cos qz & -\sin qz & 0 \\ -\sin qz & -\cos qz & 0 \\ 0 & 0 & 0 \end{pmatrix}, \quad (7)$$

where $q = 2\pi/d_{(110)}$, $d_{(110)} = a/2^{1/2}$ and a is the dimension of the cubic unit cell. It corresponds to a left handed tensorial helix 2^+ sketched in figure 3(d). As required by the O symmetry of blue phases, this tensorial helix is invariant under the symmetry operations C_2^z and C_2^x of the two-fold axes coinciding with the z and x axes of the coordinate systems (x, y, z) chosen for the particular (110) facet considered. Two other components with the same wavevector $q = 2\pi 2^{1/2}/a$ are allowed by the point group O. One corresponds to a right handed 2^- tensorial helix analogous to the other (see equation (7)); however, due to the chirality of blue phases, its amplitude $\varepsilon_{(110)}^{2^-}$ is much smaller than $\varepsilon_{(110)}^{2^+}$. The second component allowed by the O symmetry shown in figure 3(b), is also assumed to be negligible. The $\varepsilon_{(110)}^{1^+}$ (see figure 3(c)) and $\varepsilon_{(110)}^{1^-}$ tensorial helices are not invariant under π rotation C_2^z and so they must vanish.

In the local coordinate system (x, y, z) , an electric field in an arbitrary direction is

$$\mathbf{E}: (\sin \theta \cos \phi, \sin \theta \sin \phi, \cos \theta). \quad (8)$$

The dielectric energy density of the $\varepsilon_{(110)}^{2^+}$ Fourier component is

$$F^{e1}(z) = \frac{1}{8\pi} \varepsilon_{(110)}^{2^+} E^2 \sin^2 \theta \cos(qz + 2\phi). \quad (9)$$

In order to minimize the total free energy, the crystal–isotropic liquid interface occurs at discrete levels such that the last slab of thickness $d_{(110)}/2$ in the vicinity of the interface has a negative dielectric energy $F^{e1}(z)$ (see equation (9)). It was shown in [4] that the periodic potential of equations (1) and (2) can be expressed as

$$\begin{aligned} V(E, z) &= \frac{1}{8\pi q} \varepsilon_{(110)}^{2^+} E^2 \sin^2 \theta \sin(qz + 2\phi) \\ &= V_E \sin^2 \theta \sin(qz + 2\phi). \end{aligned} \quad (10)$$

The superposition of $V(0, z)$ and $V(E, z)$ is then simply

$$V_{\text{eff}}(z) = V_{\text{eff}} \sin(qz + \psi), \quad (11)$$

where the amplitude V_{eff} of the effective potential $V_{\text{eff}}(z)$ is

$$V_{\text{eff}}^2 = V_0^2 + 2V_0 V_E \sin^2 \theta \cos(2\phi - \phi_0) + V_E^2 \sin^4 \theta. \quad (12)$$

The step energy (per unit length in the y direction) $\beta_{(110)}^{\text{eff}}$ corresponding to this effective potential can be calculated as [1]

$$\beta_{(110)}^{\text{eff}} = 8q^{-1} (V_{\text{eff}} \gamma_0)^{1/2}. \quad (13)$$

We introduce a dimensionless quantity

$$\begin{aligned} \tilde{\beta}_a &= \left(\frac{\beta_{(110)}^{\text{eff}}}{\beta_{(110)}^0} \right)^4 - 1 \\ &= \frac{V_{\text{eff}}^2}{V_0^2} - 1, \end{aligned} \quad (14)$$

which is zero without the field and measures the modification of the step energy due to the field.

Using equations (14) and (12) we obtain, explicitly,

$$\tilde{\beta}_a = 2 \frac{V_E}{V_0} \sin^2 \theta \cos(2\phi - \phi_0) + O\left(\frac{V_E^2}{V_0^2}\right). \tag{15}$$

Obviously, β_a depends on the intensity $|\mathbf{E}|$ as well as on the orientation of the field, with respect to the local coordinate system (x, y, z) , given by the angles θ and ϕ . For a given direction of the field in the laboratory referenced frame, θ and ϕ are calculated in each of 12 local reference frames $(x, y, z)_n$ chosen in the same way for each of the

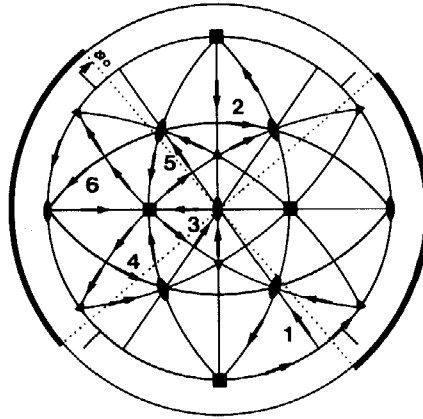


Figure 4. Stereogram used for the calculation of the field direction with respect to the local coordinates $(x, y, z)_n$ of each of the visible facets 1–6. The two-fold axis in the centre of the stereogram coincides with the z_n axis of the n th facet. The two-fold axis situated in the E–W direction, perpendicular to z_n , coincides with the x_n axis of the n th facet. The trajectory of the electric field varying along **OA**, **OB**, **OC**, **OA**, **OD** and **OC** directions (see figure 1), as seen in the reference frame $(x, y, z)_n$ of the n th facet, forms an n th loop, indicated by arrows made of sections of great circles.

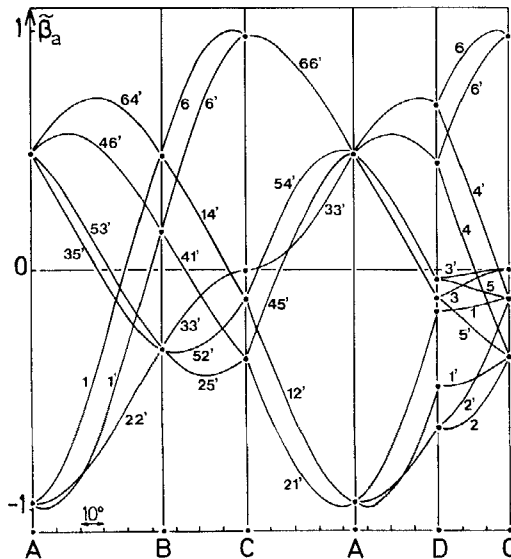


Figure 5. Variation of the quantity $\tilde{\beta}_a$ on the loop ABCADC calculated for all facets of the crystal shape shown in figure 1.

12 facets $\{1, 2, \dots, 6, 1', \dots, 6'\}$. For this purpose it is convenient to use the stereogram of figure 4. Its principle is the following. Let us suppose first that the field is directed along the four-fold axis \mathbf{OA} (see figure 1). In the reference frame $\{x, y, z\}_3$ of facet 3, this four-fold axis is on the left of the two-fold axis ($\parallel z_3$) in the centre of the stereogram. For a field varying along the loop ABCADC (see §2), the corresponding field directions form loop 3 (indicated by arrows) which is composed of sections of great circles. In the reference frame of other facets, the field trajectory corresponding to other loops are also indicated in the stereogram.

Using this representation we calculate $\tilde{\beta}_a(\theta_n, \phi_n)$ in the limit of low field, where the last term in equation (15) is neglected, and for an arbitrarily chosen value of the phase, $\phi_0 = 5^\circ$. The variation of $\tilde{\beta}_a(\theta_n, \phi_n)$ on the loop ABCADC is shown in figure 5.

4. Discussion

As far as symmetry reduction is concerned, figure 5 does not provide new information. As expected from the considerations of §2, $\tilde{\beta}_a$ is the same for all facets belonging to the same subset of equivalent facets (third column of the table). The new result concerns the relative position of branches (corresponding to different subsets of facets) with respect to each other and an isotropic level $\tilde{\beta}_a = 0$ (for $\mathbf{E} = \mathbf{0}$). For example, when the field is directed along the four-fold axis \mathbf{OA} $\tilde{\beta}_a$ is positive for facets of the subset $S_1^A = \{3, 4, 5, 6, 3', 4', 5', 6'\}$ and negative for the facets of the subset $S_2^A = \{1, 2, 1', 2'\}$.

The inequality

$$\tilde{\beta}_a(S_1^A) > 0 > \tilde{\beta}_a(S_2^A) \tag{16}$$

does not depend on the value of the amplitude e_{110}^{2+} (except for a sign change) nor on the length $|\mathbf{q}|^{-1}$ of the wavevector but is modified by a different choice of phase, ϕ_0

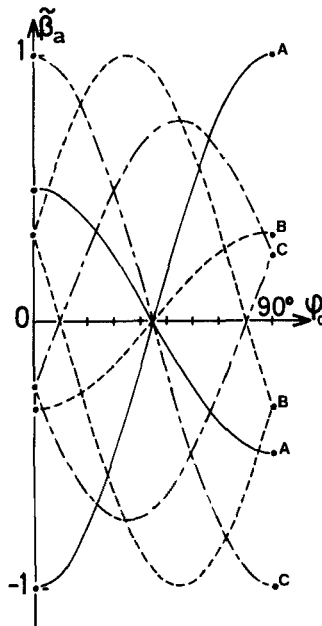


Figure 6. Variation of $\tilde{\beta}_a$ of different branches in points, A, B and C of figure 5 versus the phase ϕ_0 .

(our initial choice $\phi_0 = 5^\circ$ was arbitrary). In order to check the variation of the relative positions of different branches, in points A, B and C of figure 5, as a function of ϕ_0 , we plot $\tilde{\beta}_a(\phi_0)$ in figure 6. When $\mathbf{E} \parallel \mathbf{OA}$ we have

$$\text{and } \left. \begin{aligned} \tilde{\beta}_a(S_1^A) > 0 > \tilde{\beta}_a(S_2^A) \quad \text{for } 0 < \phi_0 < 45^\circ \\ \tilde{\beta}_a(S_2^A) > 0 > \tilde{\beta}_a(S_1^A) \quad \text{for } 45^\circ < \phi_0 < 90^\circ, \end{aligned} \right\} \quad (17)$$

so that the behaviour of the facets of the subsets S_1^A and S_2^A interchange. Similar inversions occur for other directions of the field (B and C of figure 6). The choice of the phase ϕ_0 is, therefore, a parameter of this theory which can be determined if we know how different facets behave for different directions of the field.

5. Observations of crystal shapes in the field

(110) facets are present on crystals of both blue phases [6–8]. For the purpose of this paper it is more convenient to consider only the blue phase II because its growth forms only exhibit (110) facets when $\mathbf{E} = \mathbf{0}$.

Blue phase II crystals nucleate preferentially with their two-fold, three-fold and four-fold axes perpendicular to the cell surfaces (shown in figure 7) made of two parallel glass plates coated with transparent electrodes. Since the field is perpendicular to the electrodes in this geometry three different orientations $\mathbf{OA} \parallel \mathbf{E}$, $\mathbf{OB} \parallel \mathbf{E}$ and $\mathbf{OC} \parallel \mathbf{E}$ are available. It is important to note that only the orientation $\mathbf{OA} \parallel \mathbf{E}$ is absolutely stable. As pointed out in [9], the two other orientations are unstable. When the field intensity $|\mathbf{E}|$ is larger than thresholds $E_c^{\mathbf{OB}}$ and $E_c^{\mathbf{OC}}$, the crystallites are reoriented so that the four-fold axis \mathbf{OA} is parallel to the field. In the present experiments, we have maintained $|\mathbf{E}|$ below these thresholds.

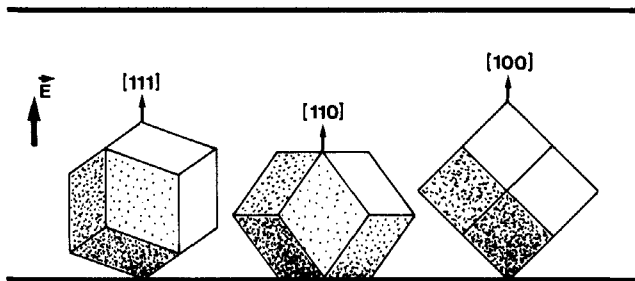


Figure 7. Spontaneous orientations of BP II crystals.

The sample was a mixture of CB15 in E9. We have grown crystals of different orientations with and without a field $E = 4 \text{ kV cm}^{-1}$. Figure 8 summarizes our observations of crystal shapes. In the geometry $\mathbf{E} \parallel \mathbf{OB}$ (see figure 8(c)), we have observed $\{1,1',4,4',6,6'\}$ facets (see figure 1) parallel to the field. The growth rate of three facets of the subset $S_1^B = \{1,6,4'\}$ was much larger in the field than that of facets of the subset $S_2^B = \{1',6',4\}$. Consequently, facets of the subset S_2^B are much larger on the growth form than facets of the subset S_1^B . As far as a possible value of the phase ϕ_0 is concerned, this experimental result means that $\phi_0 \neq 90^\circ$. Furthermore the growth of the facets of the subset S_2^B is slower in the field than without the field, suggesting that $\phi_0 > 10^\circ$. In the geometry of figure 8(d) ($\mathbf{E} \parallel \mathbf{OC}$) we have observed

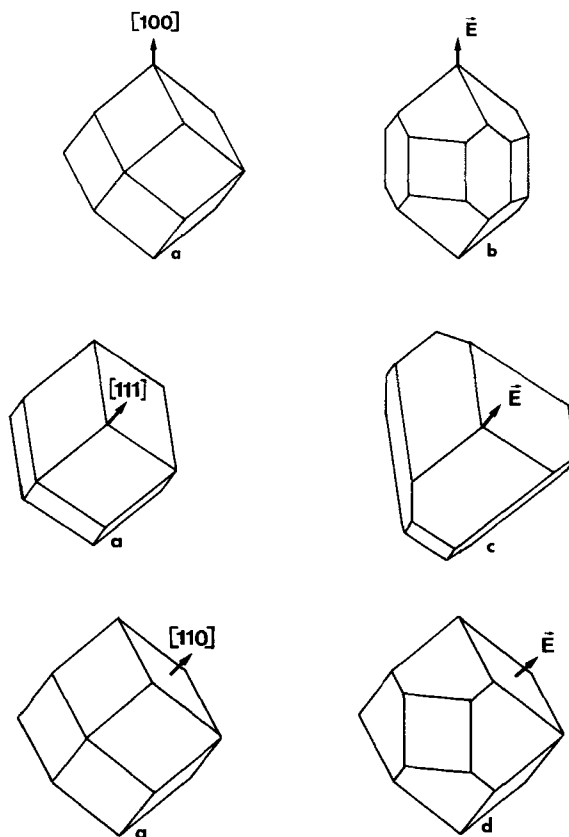


Figure 8. Crystals of the blue phase II grown (a) without and (b) with the field $\mathbf{E} \parallel \mathbf{OA}$, (c) $\mathbf{E} \parallel \mathbf{OB}$ (d) $\mathbf{E} \parallel \mathbf{OC}$.

that the 6 and 6' facets are blocked by the field (their growth rate decreases in the field). Using figure 6 we find that ϕ_0 must be $< 45^\circ$. Without any quantitative measurements of the growth rates we can conclude that the phase ϕ_0 must satisfy the inequality

$$10^\circ < \phi_0 < 45^\circ. \quad (18)$$

Another interesting feature of the crystal shapes shown in figures 8 (b) and 8 (c) is the appearance of (100) facets. This drastic modification of growth forms was explained in a previous article [4] as due to the helicoidal character of the four-fold axis of symmetry 4. The appearance of these new facets modifies shapes of the adjacent (110) facets but, as required, the modification obeys the symmetry considerations discussed in §2.

5. Conclusions

An applied electric field breaks spatial isotropy so, at equilibrium, only those crystal shapes compatible with this reduced symmetry grow. This effect is small for atomic crystals but has been observed in blue phase crystals which have millions of molecules per unit cell.

References

- [1] NOZIERS, P., 1983–1984, Lectures on crystal shapes, Collège de France.
- [2] ROTTMAN, C., and WORTIS, M., 1984, *Phys. Rev.*, **103**, 59.
- [3] SCHULZ, H., 1985, *J. Phys., Paris*, **46**, 257.
- [4] PIERANSKI, P., CLADIS, P. E., and BARBET-MASSIN, R., 1986, *J. Phys., Paris*, **47**, 129.
- [5] GREBEL, H., HORNREICH, R. M., and SHTRIKMAN, S., 1983, *Phys. Rev. A*, **28**, 1114.
- [6] BLÜMEL, T., and STEGEMEYER, H., 1984, *J. Crystal Growth*, **66**, 163.
- [7] BARBET-MASSIN, R., CLADIS, P. E., and PIERANSKI, P., 1984, *Phys. Rev. A*, **30**, 1161.
- [8] PIERANSKI, P., CLADIS, P. E., and BARBET-MASSIN, R., 1985, *Phys. Rev. A*, **31**, 3912.
- [9] PIERANSKI, P., CLADIS, P. E., GAREL, T., and BARBET-MASSIN, P., 1986, *J. Phys., Paris*, **47**, 139.